Morphology, Dynamic Mechanical, and Electrical Properties of Bio-Based Poly(trimethylene terephthalate) Blends, Part 2: Poly(trimethylene terephthalate)/Poly(ether esteramide)/Polycarbonate Blends

Toshikazu Kobayashi,[1] Barbara A. Wood,[2] Akio Takemura[3]

[1]*Engineering Polymers, DuPont Co., Wilmington, Delaware 19880-0323*
[2]*Central Research and Development, DuPont Co., Wilmington, Delaware 19880-0323*
[3]*Laboratory of Polymeric Materials, Department of Biomaterial Sciences, Graduate School of Agricultural and Life Sciences, University of Tokyo, 1-1-1 Yayoi, Bunkyo-ku, Tokyo 113-8567, Japan*

Received 15 July 2010; accepted 25 March 2011
DOI 10.1002/app.34571
Published online 9 August 2011 in Wiley Online Library (wileyonlinelibrary.com).

ABSTRACT: Bio-based poly(trimethylene terephthalate) (PTT) and poly(ether esteramide) (PEEA) blends were prepared by melt processing with varying weight ratios (0–20 wt %) of polycarbonate (PC). The blends were characterized by differential scanning calorimetry (DSC), dynamic mechanical analysis (DMA), polarized light microscopy (PLM), and transmission electron microscopy (TEM). Electrostatic performance was also investigated for those PTT blends since PEEA is known as an ion conductive polymer. DMA suggests that PC is miscible with PEEA and selectively goes into PEEA phase in case of ternary blends of PTT/PEEA/PC. The glass transition temperature (T_g) for PC/PEEA is well predicted by Gordon Taylor equation. Addition of PC retards the electrostatic decay performance of PTT/PEEA blends by restricting the motion of ions in PEEA through increasing the T_g of PEEA. © 2011 Wiley Periodicals, Inc. J Appl Polym Sci 123: 1056–1067, 2012

Key words: bio-based; PTT; static dissipative; ion conductive polymer; morphology; polycarbonate

INTRODUCTION

Poly(trimethylene terephthalate) (PTT) is a newly commercialized aromatic semicrystalline polyester with growing applications in fibers, films, and engineering polymers. PTT belongs to the thermoplastic aromatic polyester family, which includes poly (ethylene terephthalate) (PET) and poly(butylene terephthalate) (PBT). DuPont has recently commercialized the Sorona® PTT renewably sourced polymer which is made by polycondensation as shown in Scheme 1 from 1,3-propanediol (derived from renewable corn sugar) and fossil fuel derived terephthalic acid (TPA) or dimethyl terepthalate (DMT). The diol component of this polymer, 1,3-propanediol, can be manufactured via a biological fermentation process from corn sugar.[1–4] DuPont and Genencor International have developed a bacterial biocatalyst to convert corn-derived glucose to 1,3-propanediol in a single stage. DuPont and Tate and Lyle have developed the commercial scale manufacturing process for 1,3-propanediol based on this biocatalyst.

Bio-based polymers are generating considerable interest as alternatives to traditional petroleum-based polymers. The polymers and materials derived from mixed sources of renewables and fossil fuels not only have the desired performance but also are drawing a lot of attention from the sustainability point of view.

PTT provides all the advantages generally associated with polyesters, including excellent physical and chemical properties, dimensional stability, low moisture absorption, processability with appropriate nucleating agent, and recyclability. Before DuPont introduced bio-based PTT into the market, petroleum-based PTT was commercially available from 1988 to 2009 from Shell Corp. PTT polymer has been widely studied especially with regard to its fiber properties,[5–8] crystal structure,[9–12] and thermal and crystallization behaviors.[13–19] More recently PTT/clay nanocomposites,[20–23] PTT/carbon nanotube,[24] and polymer blends such as PTT/PET,[25–27] PTT/PBT,[26,28] PTT/PC,[29–32] PTT/EPDM,[33–35] PTT/LLDPE,[36,37] and PTT/poly(ether imide) (PEI),[38,39] have been intensively studied. However, very few studies were done for electrical properties for PTT and PTT blends.

Correspondence to: T. Kobayashi (toshikazu.kobayashi@usa.dupont.com).

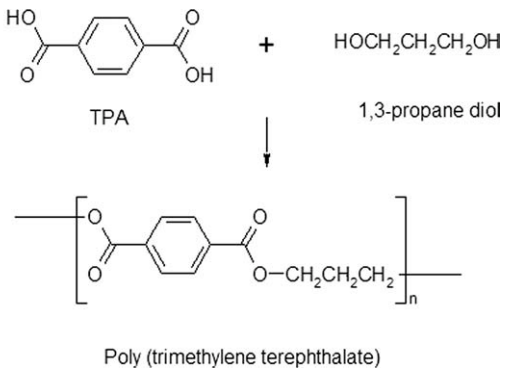

Scheme 1 PTT by condensation reaction from TPA and 1,3-propane diol.

Polymers such as polyesters and polyamides are widely used in various fields such as packaging materials, electrical/electronic parts, and automotive parts. However, the static charge that easily builds up on such molded parts from contact and/or rubbing may create the conditions for sparking and cause an electrostatic discharge, which becomes a serious problem because there may be resulting electrostatic damage to sensitive semiconductor devices and interference with circuit operation. To solve those problems, several approaches have been taken for years, such as adding low-molecular-weight surfactant or conductive fillers such as carbon black and carbon fiber. More recently, blending ion conductive polymers such as poly(ether esteramide) (PEEA) to create better static dissipative polymer systems was studied.[40–42] We recently confirmed the synergistic effect on electrostatic performance of adding ethylene copolymer based ionomers such as E/MAA-Na and E/MAA-Li into bio-based PTT blends with PEEA.[43] And it was investigated by morphological point of view. We found specific interaction between PEEA and those ionomers, which formed core-shell morphology. Those ionomers were encapsulated by PEEA, resulting higher surface area of PEEA, which enhanced the anti static performance for the ternary blends of PTT/PEEA/ionomers. We also investigated T_g effect of PEEA domain on the static dissipation performance for various PTT/PEEA blends.

Through our attempt to reduce the T_g of PEEA domain, we found polyethylene glycol 400 bis(2-ethylhexanoate) worked to reduce the T_g of PEEA by melt extrusion process technique.[44] We confirmed that static dissipative performance of the blends was significantly improved by reducing the T_g for PEEA in the blends. We believe it is explained by enhancing the ion mobility in PEEA domains through reducing the glass transition temperature of PEEA which is an ion conductive polymer. This article is focusing on how the static dissipative performance of the polymer blends change when the T_g of PEEA domain is shifted to higher temperature. Through our repeated experiments, we found polycarbonate (PC) is miscible with PEEA and increase the T_g of PEEA during the melt extrusion of PTT/PEEA/PC ternary polymer blends. Thus, we selected PC for PTT/PEEA blends to reinforce our hypothesis regarding T_g effect of PEEA domain on electro static dissipative performance.

EXPERIMENTAL

Materials

PTT (Sorona® by DuPont, intrinsic viscosity: 1.02 dL/g) and PEEA (Pelestat® 6321 M_w = 84,200) used in this work were commercial polymers manufactured by DuPont, and Sanyo Chemical Corp., respectively. The polymers were used without any purification. Sorona® polymer is manufactured from 1,3-propanediol and DMT on a commercial scale using a continuous polymerization process.[45,46] PC (Lexan PC 101, MFR 7.0 g/10 min at 300°C with 1.2 kg) was supplied by Sabic Corp. The polymers were used without any purification. Pelestat 6321 is confirmed to contain 275 ppm of Na by inductively coupled plasma (ICP) emission spectrochemical analysis.

PEEA used here is polymerized from carboxylic acid end Nylon 6 oligomer and ethoxylated Bisphenol A as shown in Scheme 2. It was identified by ^{1}H-NMR (500 MHz in DMSO-*d*6) to be composed of Polyethylene Glycol (PEG)/Bisphenol A/Nylon 6/TPA (44.2/6.8/44.1/4.9 in wt %). The chemical structure for PC is shown in Scheme 3.

Sample preparation

PTT pellets, PEEA pellets, and PC pellets were premixed and extruded on a ZSK 30 twin screw extruder using a barrel set temperature of 250°C and a screw speed of 300 rpm with the vacuum vent port applied for all formulations. The melt blended samples were PTT/10% PEEA, PTT/10% PC, PTT/10% PEEA/5% PC, PTT/10% PEEA/10% PC, and PTT/10% PEEA/20% PC.

The extruded strand was cut into pellets for injection molding. The extruded pellets were dried for 2 h at 135°C before molding and molded into 7.5 cm × 12.5 cm × 3.2 mm plaques, ASTM tensile test bars and flexural test bars using an injection molding machine (Sumitomo J-150). The set temperatures for the cylinder and the mold were 250°C and 50°C, respectively.

Measurement

A differential scanning calorimeter, TA Instruments Q1000 MDSC (modulated DSC) operating in

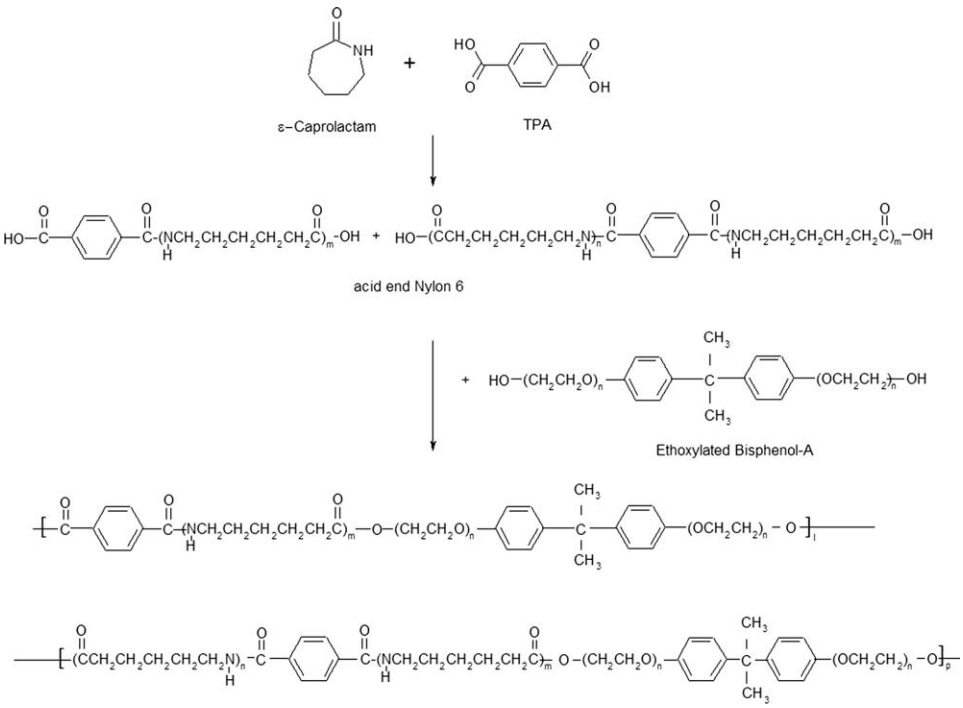

Scheme 2 PEEA by condensation reaction from carboxylic acid end Nylon 6 and ethoxylated Bisphenol A.

"Standard Mode," was used to determine the cold crystallization and recrystallization peaks in a melt quenched sample of the thermoplastic composition. A 10–12 mg sample of the composition was weighed into an aluminum DSC pan and the sample heated to 280°C in a DSC for 10 min under nitrogen atmosphere to provide an equilibrated melt sample. The melt sample was removed from the DSC and quick quenched by immersing the sample in liquid nitrogen. The melt quenched sample was equilibrated at 0°C in the DSC under nitrogen atmosphere, followed by heating at 10 °C/min scan rate to 280°C; held at isothermal for 3 min at 280°C, and cooled at 10 °C/min scan rate to 30°C; while recording the thermal events. The cold crystallization peak is the first exothermic peak exhibited in the heating cycle, having a peak height maximum at about 65–75°C. The enthalpy of the recrystallization peak was measured in Joules per gram (J/g). Peak temperatures of the exothermic curves obtained during the cooling scan were defined as the crystallization temperature (T_c). From the exothermic heat of ΔH which is caused by crystallization, the crystallinity is PTT is estimated with the following equation:

$$\text{Crystallinity} = \Delta H/\Delta H^0 \quad (1)$$

where ΔH^0 is the fusion of 100% crystalline polymer. Exothermic heats were normalized by the polymer weight percentage in the crystallinity calculations.

Transmission electron microscopy (TEM) was performed on ultrathin sections taken from molded tensile bars. To mark the molded surface, the bars were painted with a liquid epoxy mixture which was cured overnight at 60°C. Cryoultramicrotomy with diamond knives was carried out at −90°C to produce sections of nominal thickness 90 nm. Sections were examined both unstained and after 2 h exposure to RuO_4 vapor. Images were obtained using a JEOL 2000FX TEM operated at 200 kV accelerating voltage and recorded on a digital camera.

A Nikon Microphot-FX polarized microscope was used in conjunction with a Linkam THM 600 hot stage. The stage equipped with a Linkam TMS-90 temperature control system allowed samples to be heated and cooled at adjustable rate. The digital video photograph system of PLM includes Panasonic Digital 5000 CCD color video camera, color video monitor, and DVD recorder.

Dynamic mechanical analysis was performed on the samples of 40 mm × 28 mm × 4 mm in size using a dynamic mechanical analyzer (2980 DMA, TA Instruments) under a single cantilever mode in a temperature range from −150 to 150°C at a constant heating rate of 2 °C/min, and at frequency of 2 Hz. All the specimens were annealed at 80°C for 30 min before the testing.

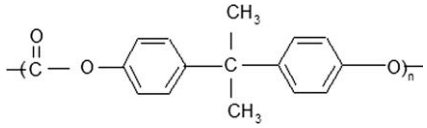

Scheme 3 Polycarbonate.

TABLE I
Thermal Properties for Various PTT/PEEA/PC Blends

Recipe	Heating				Cooling			
	T_g (°C)	T_{cc} (°C)	ΔH_{cc} (J/g)	T_m (°C)	T_c (°C)	ΔH_c (J/g)	ΔT_c (T_{onset}-T_c) (°C)	Crystalline degree (%)
PTT	45.9	72.4	36.5	229.1	172.6	45.4	17.2	31.2
PTT/10% PEEA	45.1	70.8	43.6	227.7	165.9	42.5	23.5	32.4
PTT/10% PEEA/5%PC	46.2	72.6	35.2	226.5	157.4	39.5	28.5	31.9
PTT/10% PEEA/10%PC	44.2	74.8	35.3	225.9	146.4	34.9	33.4	30.0
PTT/10% PEEA/20%PC	46.6	82.7	32.2	225.5	128.8	26.0	37.4	25.5
PTT/10%PC	49.3	78.3	39.3	227.0	156.1	41.5	27.4	31.7
PTT/10%PC 2nd cycle		–		224.1	136.4	32.2	36.1	24.6
PTT/10%PC 3rd cycle		95.4	10.5	215.4	121.6	11.9	38.7	9.1

Static charge dissipation was measured at 23°C and 50% R.H on Static Honest Meter *S*-4104 (Shishido Shokai Co., Tokyo, Japan) after applying 10 kV of corona discharge for 60 s. Static Honest Meter is a measuring instrument for attenuation of static electricity. This device is used to electrify the specimen by irradiating it with air ions generated by corona discharges initiated by the device, and then, after the irradiation is stopped, it is used to investigate the decay curve of the charge on the specimen. All samples were conditioned with 23°C and 50% R.H. for 48 h prior to the testing. Surface resistivity values were measured according to ASTM D-257.

RESULTS AND DISCUSSION

Differential scanning calorimetry

The crystallization rate for PTT and PTT blends studied here can be compared by the crystallizing temperature (T_c) and the half peak width of the crystallization peak (ΔT_c). The higher the T_c peak temperature and the narrower the ΔT_c width are, the faster the crystallization rate is. Table I lists the analyzed values obtained in the DSC measurements for various PTT blends studied here. The heating scan DSC for the quick quenched sample by liquid nitrogen is shown in Figure 1. The glass transition temperature (T_g) for both neat PTT and ternary blends of PTT/PEEA/PC is shown around 45°C. PTT/10% PC shows the glass transition at 49°C, which is shifted to higher temperature. The cold crystallization peak on heating up to the melt (T_{cc}), which is observed as an exothermic peak, was shown at 72.4°C for neat PTT. The exothermic peak enthalpy (ΔH_c) for the various PTT blends are shown in Table I. T_{cc} for the PTT blends shifts to higher temperature with increasing PC content. PTT/10% PEEA/20% PC has T_{cc} at 82.7°C which is 10°C higher than that of neat PTT. This suggests that the mobility of the molecular chain needed for recrystallization is restricted, although the T_g for PTT/10% PEEA/20% PC observed by DSC is about the same as for neat PTT. The cooling scan DSC is shown in Figure 2. The crystallization peak (T_c) for neat PTT can be seen at 172.6°C. When PEEA is added into PTT, T_c shifts to lower temperature (165.9°C for 10% addition) and the exothermic peak width (ΔT_c: $T_{onset} - T_c$) becomes broader from 17.2°C to 23.5°C, which

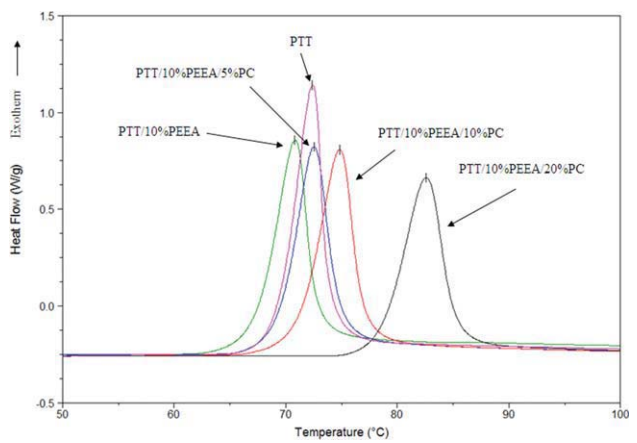

Figure 1 DSC heating scan for PTT and PTT blends. [Color figure can be viewed in the online issue, which is available at wileyonlinelibrary.com.]

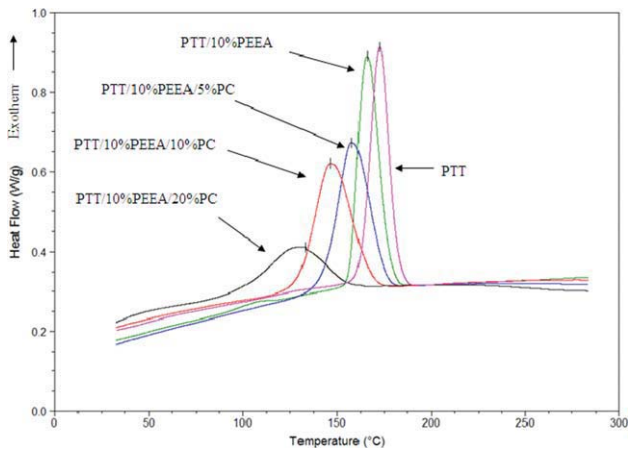

Figure 2 DSC cooling scan for PTT and PTT blends. [Color figure can be viewed in the online issue, which is available at wileyonlinelibrary.com.]

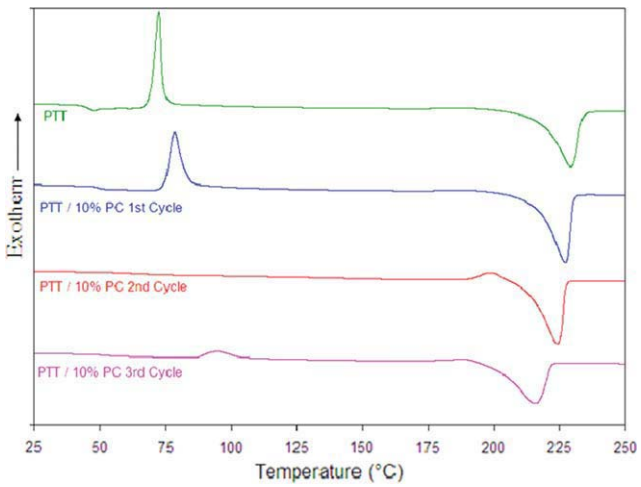

Figure 3 DSC heating scan for PTT/10% PC with multiple heating and cooling cycles. [Color figure can be viewed in the online issue, which is available at wileyonlinelibrary.com.]

suggests that PEEA retards the crystallization rate for PTT and acted as a denucleant. T_c shifts to lower temperature with increasing PC content, and ΔT_c becomes broader as shown in Figure 2, which indicates that PC also retards the crystallization rate for PTT. Figure 3 shows DSC heating scan for PTT/10% PC with three cycles. One cycle means heating the sample at 10 °C/min up to 280°C, holding for 3 min, and cooling at 10 °C/min. The first cycle scan is the sample after rapid quenching by liquid nitrogen, 2nd and 3rd cycle are without any rapid quenching procedure. The first cycle for PTT/10% PC shows T_{cc} at 78.3°C, which is 5.7°C higher than T_{cc} for neat PTT. The second heating scan does not show any cold crystallization, which means that the sample

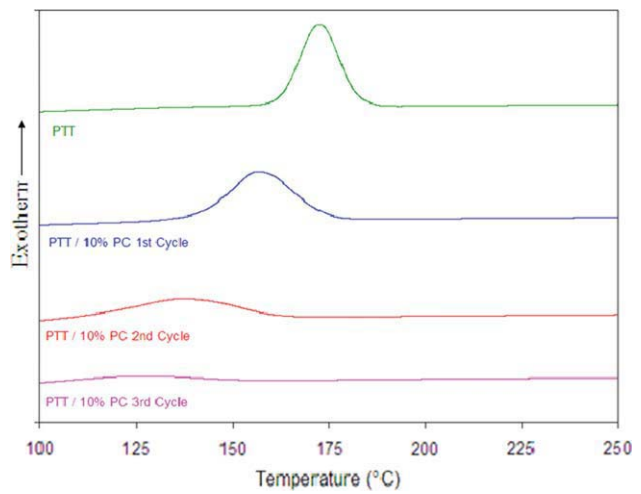

Figure 4 DSC cooling scan for PTT/10% PC with multiple heating and cooling cycles. [Color figure can be viewed in the online issue, which is available at wileyonlinelibrary.com.]

crystallized during the first cycle cooling process. The third cycle scan, however, shows 10.5 J/g of exothermic peak at 95.4°C, which indicates the rate of crystallization became slow and therefore the crystallization was incomplete during the second cycle cooling process. The melting peak (T_m) for the three cycles changed form 227.0°C to 224.1°C, and 215.4°C, which suggests that a copolymer is generated by transesterification between PTT and PC. Figure 4 shows the DSC cooling scan for PTT/10% PC with three cycles. The T_c shifts to lower temperature and ΔT_c ($T_{\text{onset}} - Tc$) becomes broader, which is explained by slower rate of crystallization of PTT on addition of PC. The crystallinity for PTT with the previously described DSC conditions was calculated as 31.2% from the cooling scan which is in good agreement with Zhang.[47] Normalized crystallinity of the PTT portion for various PTT blends are shown in Table I. The value for ΔH^0 in the eq. (1) is 30 kJ/mol = 145.5 J/g as determined by Pyda et al.[48] ΔH_c for PTT/10% PC blend becomes smaller, its crystallinity also changed from 31.7% to only 9.1% for the first cycle versus third cycle as shown in Table I. All the phenomena observed here suggest that PTT and PC becomes more and more miscible through transesterification with repeated melting, which has good agreement with previous studies done by Xue et al., Aravind et al., and Yavari et al.[29,49,50] Very similar phenomena were also reported for PET/PC[51] and PBT/PC.[52]

Dynamic mechanical analysis

Dynamic mechanical heating scans were performed with bars described in the experimental section.

Figure 5 shows tan δ for neat PTT and PTT blends within the temperature range −150 to 50°C, and the β-relaxation for neat PTT can be observed at −71.2°C. Early studies indicated that the β-relaxation is produced by joint movement of phenyl rings and

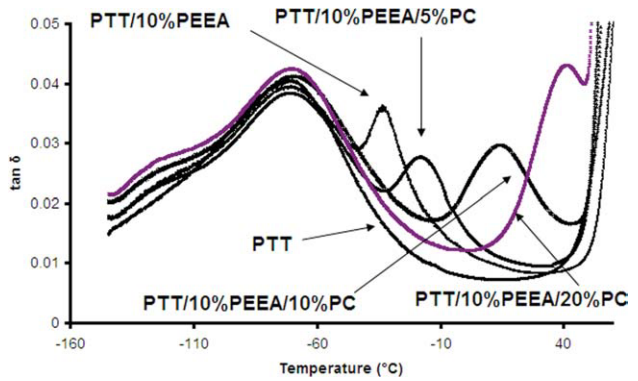

Figure 5 DMA for PTT blends (tan δ versus temperature): −150 to 60°C. [Color figure can be viewed in the online issue, which is available at wileyonlinelibrary.com.]

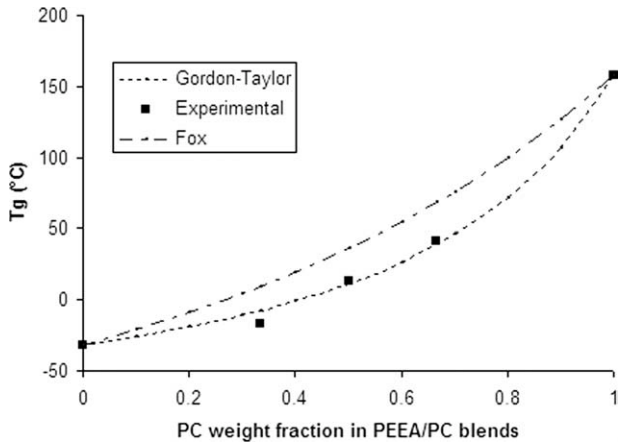

Figure 6 T_g of PEEA/PC blends as the function of blend composition.

carbonyl entities.[53–57] The β-relaxation for PTT is basically unchanged when PEEA and PC are added. As shown in Figure 5, T_g for PEEA is observed at −32°C for PTT/10% PEEA blend, and it moves to −17°C, 14°C, and 41°C when the amount of PC into PTT/10% PEEA increases to 5%, 10, and 20%, respectively. We do not see any separate α-relaxation peak for PC although neat PC shows an α-relaxation peak at 158°C with this DMA testing condition. Judging from the DMA results, PEEA and PC are miscible pairs. It is probably not appropriate to draw a T_g curve for the PEEA and PC weight ratio from the ternary blends DMA results since there is no guarantee that PC and PEEA are able to complete the interaction with the PTT matrix during the limited melt processing time. Still, it seems worthwhile to plot the T_g as shown in Figure 6, where T_g for PEEA/PC blends is shown versus the weight fraction of PC. Several models have been proposed to predict the composition dependence of T_g in the miscible polymer blends. Some of these are Couchman and Karasz, [58] Fox,[59] Gordon and Taylor,[60] and Utrachi[61] equations. In the Fox model, the observed T_g of the blend is related to the T_g values of the neat components and their composition according to the following equation:

$$\frac{1}{T_g} = \frac{W_1}{T_{g1}} + \frac{W_2}{T_{g2}} \tag{2}$$

where W_1 and W_2 are the weight fraction of the components 1 and 2 having the T_g values of T_{g1} and T_{g2}, respectively. The Gordon–Taylor equation for the prediction of the composition dependence of T_g in miscible polymer blends is written as:

$$T_g = \frac{W_1 T_{g1} + k W_2 T_{g2}}{W_1 + k W_2} \tag{3}$$

where k is the fitting parameter.

Figure 6 shows the experimental data for the T_g corresponding to PEEA domain of the blends as obtained from the DMA data along with the predictions of the Fox model and the Gordon–Taylor equation with a fitting parameter of $k = 0.3$. It is clearly observed from Figure 6 that the Gordon–Taylor equation fits the experimental data better than the Fox equation. Figure 7 shows tan δ in the range from 0 to 140°C. The α-relaxation peak which corresponds to the glass transition temperature for neat PTT is observed at 79°C. T_g for PTT for all the blends studied here is basically unchanged, which support the notion that PTT and PC are immiscible with two separate phases without any extra melt mixing time.[62] Figure 6 suggests that the PC goes into the PEEA domains selectively in the PTT matrix. It is noted that PTT/10% PEEA/20% PC has double tan δ peaks at 62°C and 79°C. This phenomenon is reported when the cold crystallization of the PTT sample occurs during the DMA.[20,22,63] As shown in Figure 2, the DSC heating scan for the quenched samples, PTT/10% PEEA/20% PC shows the cold crystallization peak at 82°C. Therefore, annealing at 80°C for 30 min is not enough to eliminate the cold crystallization. Figure 8 shows the DMA of PTT/10% PEEA/20% PC with 100°C, 30 min annealing. The double peak has disappeared and a single peak is now observed at 89°C for tan δ of PTT. The miscibility between PTT and PC is greatly enhanced by the occurrence of transesterification when the mixing time is longer than that of normal melt compounding process.[64,65] It is also notable that the T_g for PEEA shifted to 27°C from 41°C. Considering both observations together, it is reasonable to conclude that PC located at the interface between PTT and PEEA domains becomes more miscible with PTT and consequently it is pulled away from PEEA domains. It is surprising to see the miscibility change between PTT and PC during the

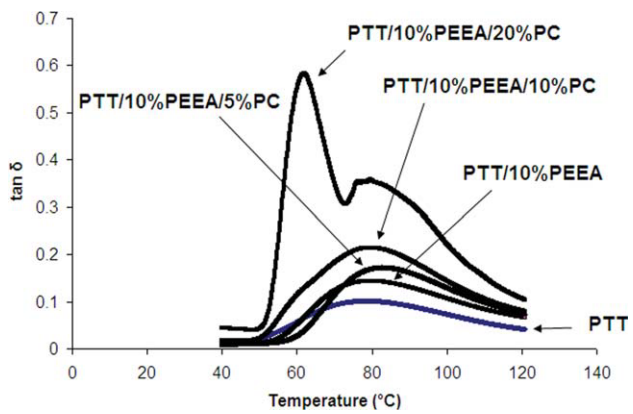

Figure 7 DMA for PTT blends (tan δ versus temperature): 40–120°C. [Color figure can be viewed in the online issue, which is available at wileyonlinelibrary.com.]

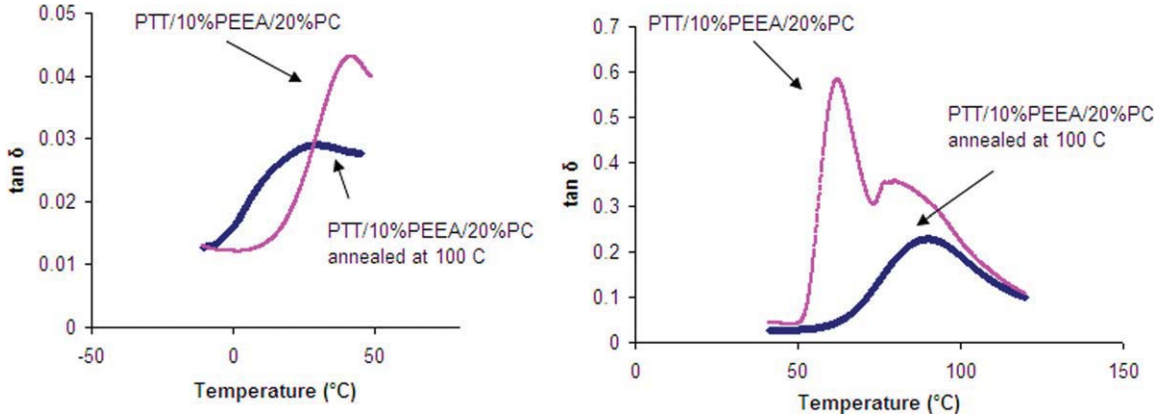

Figure 8 DMA for PTT/10% PEEA/20% PC annealed at 100°C (tan δ versus temperature). Left: −20–50°C, Right: 40–120°C. [Color figure can be viewed in the online issue, which is available at wileyonlinelibrary.com.]

100°C solid-state annealing treatment. Those DMA results are summarized in Table II.

One of the desirable end-use characteristics of the PTT/PEEA blend would be electrostatic dissipative performance due to the ion conductive nature of PEEA. The T_g of the PEEA domains influences its electrostatic performance, which is discussed in electrical properties section below.

Spherulite morphology

An optical microscope equipped with a digital video photography system was used to monitor the transmitted light image of the spherulite growth of PTT and PTT blends recrystallized from the melt under controlled conditions.

Figure 9 shows the cross-polarized light optical microscopy (PLM) images spherulites with the distinctive Maltese cross pattern of extinctions. These spherulites were grown by nonisothermal crystallization at the same cooling rate (10 °C/min) as DSC after holding the specimen well above the melting point of PTT at 280°C for 3 min. with the intent of "erasing" any previous thermal history. The average spherulite size for recrystallized neat PTT is about 100 μm in diameter. PTT/10% PEEA has much larger spherulites than neat PTT, averaging about 300 μm in diameter, which indicates that PEEA suppresses nucleation for PTT. This PLM image is in good agreement with the DSC results. With addition of 5 and 10% PC into PTT/10% PEEA, the spherulite formation on cooling of the melt monitor occurred at temperatures about 10°C and 17°C lower temperature than for the binary blend PTT/10%PEEA. The ternary blend containing 5% PC has spherulites of average diameter 350 μm. PTT/10% PEEA/20% PC has significantly slower crystallization speed with fewer nucleation points resulting in spherulites around 400 μm diameter.

Surface charge decay

PEEA is known as an ion conductive polymer and is commercially available as a polymeric additive to add antistatic characteristics to polymers. We previously investigated electrostatic decay performance for PET/PEEA blends with various polymers such as E/MAA, /MAA-Na, E/MAA-Li, E/MAA-Zn,

TABLE II
Electrcal Properties for PTT Blends

	Surface charge (V) vs. Decay time (sec.)						Half dissipation time (sec.)	Serface resitivity (Ω/sq)	SDPI (V-min.)	DMA results	
	0	1	3	10	30	60				tanδ peak of PTT (°C)	tanδ peak of PEEA (°C)
PTT	2650	2650	2630	2630	2630	2620	>300	2.2E+15	2624	79	
PTT/10%PEEA	2250	2000	1470	730	300	150	6	4.8E+12	506	79.1	−32.3
PTT/10%PEEA/5%PC	2420	2300	2120	1680	1150	800	22	2.9E+13	1294	81.9	−17
PTT/10%PEEA/10%PC	2650	2570	2390	2090	1650	1440	130	1.8E+14	1783	79.1	13.6
PTT/10%PEEA/20%PC annealed	2570	2520	2460	2260	1850	1690	>300	1.5E+15	1971	62, 79	41.5
PTT/10%PEEA/20%PC										89	27.5
PTT/25%PEEA	460	200	30	10	0	0	1	6.6E+10	13	79	−31

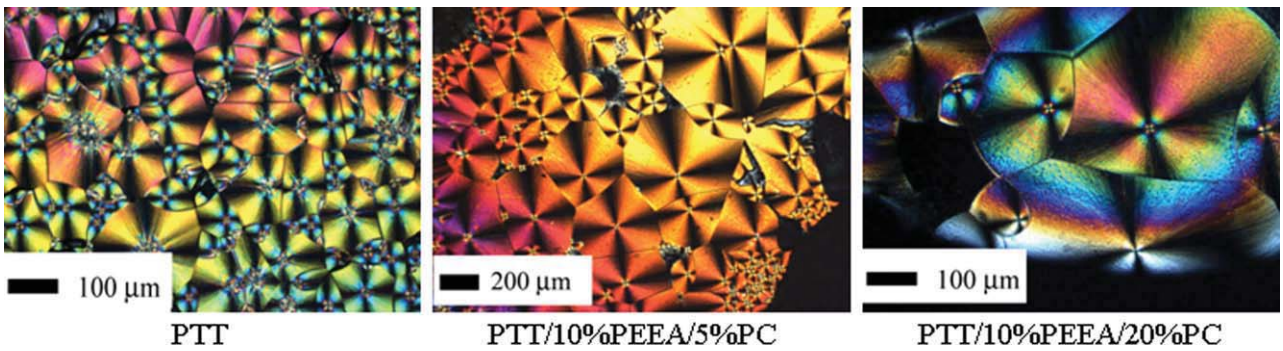

Figure 9 Polarized light microscope for PTT and PTT/PEEA/PC blends. [Color figure can be viewed in the online issue, which is available at wileyonlinelibrary.com.]

E/MAA-Mg, and polystyrene.[42] We found that the static decay performance for PET/PEEA blends can be drastically improved by adding E/MAA-Li and E/MAA-Na.

Surface charge decay curves up to 60 s for the samples were obtained by Static Honest Meter S4104 after applying 10 kV of corona discharge for 1 min. This device is used to electrify the specimen by irradiating it with air ions generated by corona discharges initiated by the device. After the irradiation is stopped, it is used to investigate the decay curve of the charge on the specimen. Static charge dissipation curve for neat PTT and PTT blends are shown in Figure 10. Neat PTT shows no dissipation during measured time of 60 s. The surface charge for PTT/10% PEEA drops from 2520 V to 150 V in 60 s. PEEA works effectively to add static dissipative characteristics to PTT by ion conductive nature of PEEA. However, when 5% of PC is added into PTT/10% PEEA, its static dissipative performance becomes worse. With further increase of PC content, the resin becomes more and more insulating material. 10% PC and 20% PC addition into PTT/10% PEEA gave 1440 V, 1690 V surface charge at 60 s, which is very slow to dissipate the surface charge. As described in the material section, the grade of PEEA studied here contains 275 ppm of Na, which works as a mobile ion in the PEEA domain. The ion movement to compensate the surface charge is the mechanism for the electrostatic dissipation. The glass transition temperature (T_g) of PEEA shifted to higher temperature as discussed in DMA section. T_g for PEEA is observed at −32°C for PTT/10%PEEA blend, and it moves to −17°C, 14°C, and 41°C when the amount of PC into PTT/10% PEEA increases to 5%, 10, and 20%. This higher T_g of PEEA suppresses rapid motion of the sodium ions through the PEEA domains, which explains why the PTT/10% PEEA blend with PC becomes more insulating like the binary blend PTT/PC as the content of PC increases.

Static decay performance index

Matsui and Kashiwamura studied the relationship between resistivity, frictional charge, and half dissipation time for antistatic fabricated fiber.[66] In their report, the concept of Index of Frictional Static Charge Dissipation was proposed to describe the antistatic performance more appropriately. It is the integral of the charge dissipation curve (2) up to 1 min after the applied friction, which is, in other words, the average static charge during 1 min multiplied by 1 min as described in eq. (3). It is known that the dissipation speed decreases when the surface charge becomes small even for the same material. Therefore, half dissipation time tends to become larger when initial surface charge of the material is low. Since good antistatic material tends to have lower initial surface charge with the same applied corona discharge, half dissipation time of the material does not always represent the antistatic performance appropriately, which sometimes makes it difficult to differentiate excellent antistatic material from others. This index is considered as a new method to describe the antistatic performance from

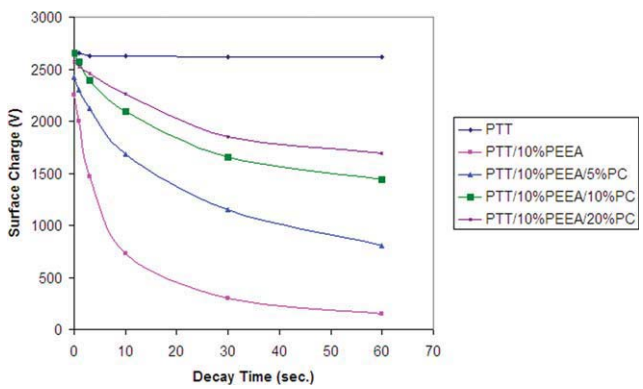

Figure 10 Static dissipation curve for PTT and PTT blends. [Color figure can be viewed in the online issue, which is available at wileyonlinelibrary.com.]

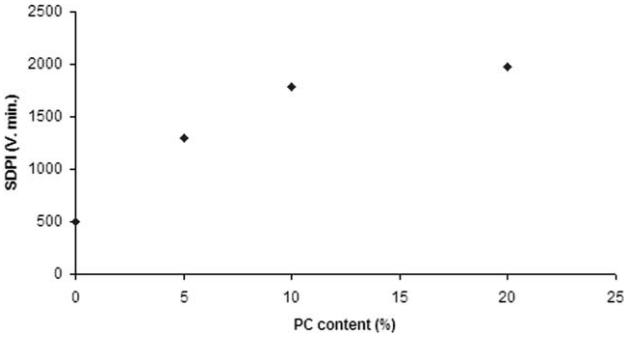

Figure 11 Static decay performance index for PTT/10% PEEA blends with 0, 5, 10, 20% PC. [Color figure can be viewed in the online issue, which is available at wileyonlinelibrary.com.]

the standpoint of both initial surface charge and decay curve. We previously applied their concept for describing static charge dissipation to discuss a broader aspect and confirmed the effectiveness of static decay performance index (SDPI).[42] The lower the SDPI value, the better static dissipative performance is achieved.

$$V = f(t) \tag{4}$$

$$\mathrm{SDPI} = \int_0^1 f(t)dt \tag{5}$$

Figure 11 shows the SDPI for the PTT blends when PEEA content is 10%. With increasing PC content, the SDPI goes up and approaches the SDPI of neat PTT, which is 2624 V min. It is very clear that PC retards the antistatic performance of PTT/PEEA. Complete data for the electrical properties such as the electrostatic dissipation, half dissipation time, and surface resistivity and SDPI is shown in Table II. The surface resistivity for PTT/10% PEEA/20% PC is measured as 1.5×10^{15} Ω/sq versus 2.2×10^{15} Ω/sq for the neat PTT resin. PTT with 10% PEEA and 25% PEEA gave 4.8×10^{12} Ω/sq, 6.6×10^{10} Ω/sq, which is consistent with electrostatic decay and SDPI performance. DMA results suggest that PEEA and PC are miscible since there is only single T_g peak for the blends. The morphological evidence to support the miscibility is discussed in the TEM section.

In our previous study, we found that E/MAA acid copolymer without any metal cation also works as a synergist for PET/PEEA blends, which suggests that the mechanism of the antistatic synergist is not

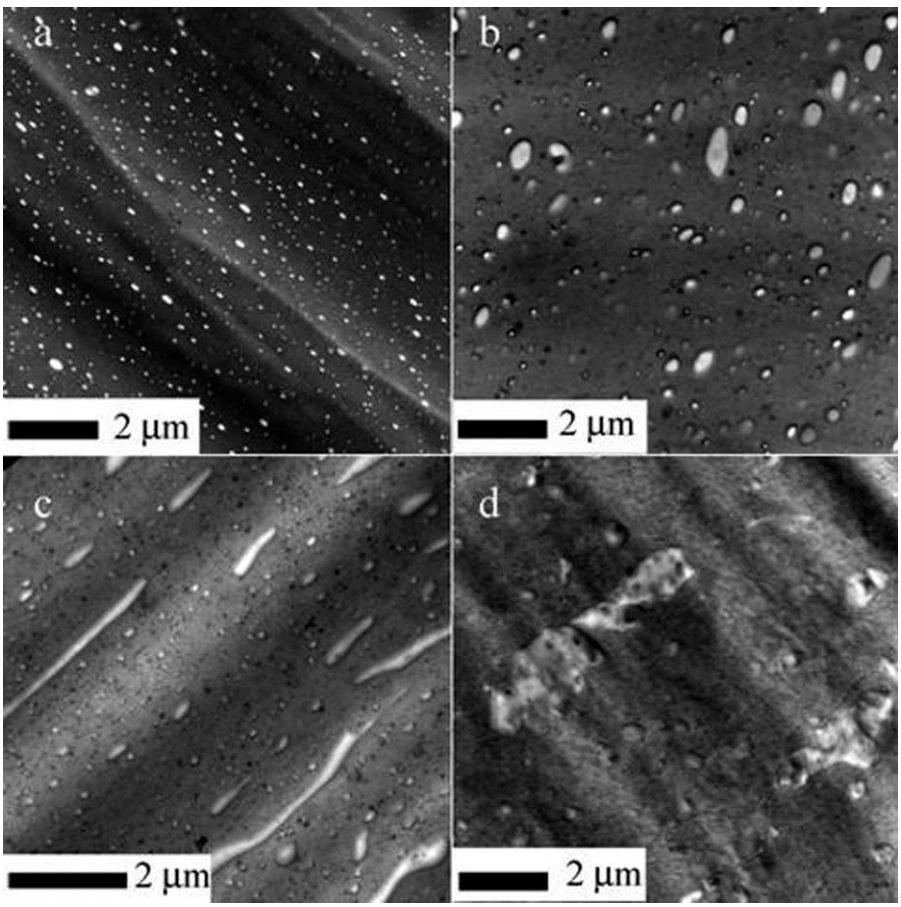

Figure 12 TEM cross-section showing subsurface region of PTT blends: (a) PTT/10% PEEA, (b) PTT/10% PEEA/5% PC, (c) PTT/10% PEEA/10% PC, (d) PTT/10% PEEA/20% PC.

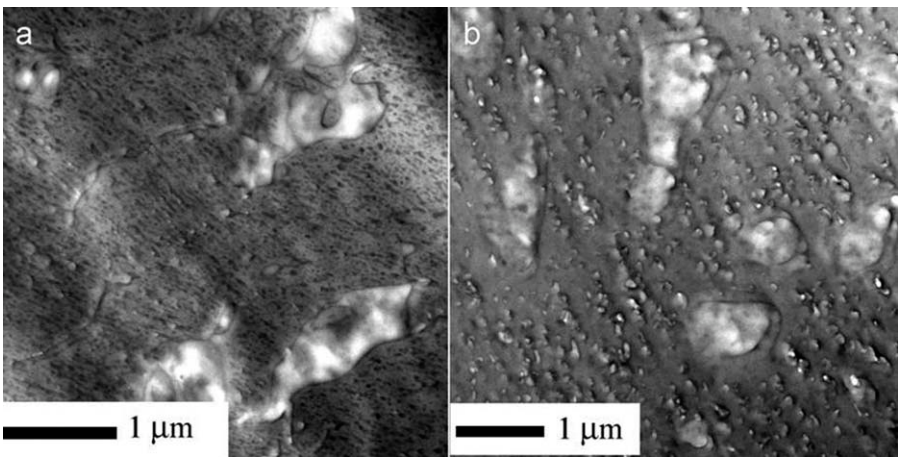

Figure 13 TEM cross-section showing subsurface region of PTT/10% PEEA/20% PC: (a) before annealing, (b) after annealing at 100°C.

cation transfer from the ionomer to PEEA but rather morphological interaction in which the PEEA encapsulates dispersed domains of the third polymer.[42] Encapsulation results in higher surface area per unit volume of PEEA compared to PET/PEEA binary blends. We also investigated T_g effect of PEEA domain on the static dissipation performance for various PTT/PEEA blends. Through our attempt to reduce the T_g of PEEA domain, we found polyethylene glycol 400 bis(2-ethylhexanoate) worked to reduce the T_g of PEEA by melt extrusion process technique.[44] We confirmed static dissipative performance of the blends was significantly improved by reducing the T_g for PEEA in the blends. We believe it is explained by enhancing the ion mobility in PEEA domains through reducing the glass transition temperature of PEEA which is an ion conductive polymer. Here we found PC retards the antistatic performance for PTT/PEEA blends by increasing the T_g of PEEA which leads restricting the ion mobility in the PEEA.

Morphology (TEM)

Bulk microstructure versus composition varies much more than near-surface microstructure from molded parts in the binary and ternary blends examined. The binary blend 90/10 PTT/PEEA was shown to contain two phases, with fairly uniform 0.2 μm dispersed phase particles [Fig. 12(a)]. The interface between the presumably pure PTT matrix and PEEA is sharp. On addition of PC to the binary PTT/PEEA blend, the dispersed phase changes contrast and shape, with particles up to almost a micron and intense staining by RuO_4 at interfaces.

Increasing the PC content results in a more diffuse interface and the appearance of some longer domains.

At the highest PC content for the ternary blend [Fig. 12 (d)], the dispersed phase structure shows a profuse amount of dark stained dots and lines, plus a few irregularly shaped blobs up to a micron in size. The large light colored domains could be comprised mostly of PC which is unable to mix with the PTT on the time scale of compounding for the molded test specimen. The bulk microstructure of the 70/10/20 PTT/PEEA/PC was observed to change after annealing at 100°C (Fig. 13.) The intense staining at PTT/PC interfaces is diminished, and interfaces appear less sharp, presumably due to migration of some of the PC into the PTT matrix. As in the DMA, which showed PEEA demixing from PC during annealing, the TEM image [Fig. 13(b)] of annealed materials shows some small white domains below 0.1 micron which resemble the pure PEEA dispersed phase seen in the binary blend PTT/PEEA shown in Figure 12(a). Images of blend material sample at or near the molded surface show a high interfacial area lamellar morphology for the 90/10/0 [Fig. 14(a)] and 85/10/5 PTT/PEEA/PC [Fig. 14(b)] compositions. Increasing the PC loading to 10% [Fig. 14(c)] or 20% [Fig. 14(d)] eliminates the strong lamellar morphology and diminishes static dissipative performance. The isolated blobs of PEEA in Figure 14(d) are inefficient for ion conduction compared to the long thin alternating planes of PTT and PEEA found at the binary blend surface. This blob morphology, in addition to the T_g increase for PEEA on PC addition, helps explain why adding PC to the binary blend PTT/PEEA deteriorates electrostatic performance.

CONCLUSIONS

Bio-based PTT and PTT blends with PEEA and PC were studied in terms of the crystallization,

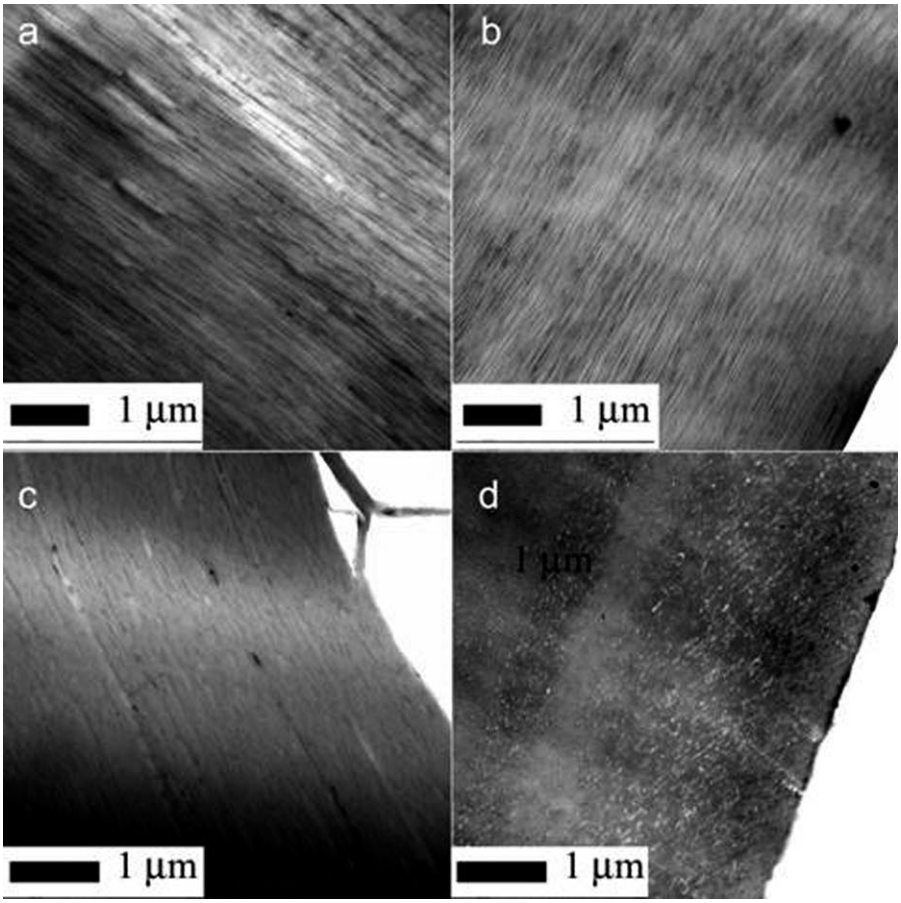

Figure 14 TEM cross-section showing molded surface of PTT blends: (a) PTT/10% PEEA, (b) PTT/10% PEEA/5% PC, (c) PTT/10% PEEA/10% PC, (d) PTT/10% PEEA/20% PC.

spherulite morphology by PLM, dynamic mechanical properties, multicomponent morphology by TEM, and electrical characteristics. DSC and DMA suggest that PTT and PC become more and more miscible with longer melt mixing or additional thermal treatment due to transesterification. DMA strongly suggests that PC and PEEA are miscible since only a single T_g peak is observed. The Gordon–Taylor equation fits the observed T_g of PC/PEEA. The morphology as observed by TEM of thin sections supports the idea that some but not all the PC becomes incorporated into a miscible blend with PTT.

SDPI, a convenient figure of merit for comparing different polymeric materials, was calculated from the electrostatic dissipation curve and it was confirmed that PEEA works effectively to reduce the SDPI for PTT. PC retards the electrostatic performance of PTT/10%PEEA by restricting the sodium ion mobility in PEEA by increasing the T_g of PEEA and by transforming the surface morphology from lamellar to isolated dispersed domains of PEEA. In other words, this study combined with our last investigation,[44] antistatic performance is significantly affected by the T_g of PEEA domain, which is an ion conductive polymer, in the polymer blends. We verified here static dissipative performance is dramatically worsened when the T_g of PEEA is increased on addition of PC.

The authors sincerely thank Steven Dunlap, Corporate Center for Analytical Science, DuPont for PLM work and Dave Gale, DuPont Engineering Polymers, and Yukio Miyagishima, Engineering Polymers Research, DuPont K.K. for the DSC and DMA measurement, and NMR analysis for Dr. Elizabeth Lozada in Corporate Center for Analytical Solutions at DuPont.

References

1. Emptage, M.; Haynie, S.; Laffend, L. A.; Pucci, J.; Whited, G. Eur. Pat. EP 1,204,755 (2001).
2. Whited, G. M.; Bulthuis, B.; Trimbur, D. E.; Gatenby, A. A. Eur. Pat. EP 1,076,708 (1999).
3. Burch, R. R.; Dorsch, R. R.; Laffend L. A.; Nagarajan, V. Int. Pat. WO 0,111,070 (2001).
4. Kurian, J. V. J Polym Environ 2005, 13, 159.
5. Grebowicz, J. S.; Brown, H.; Chuah, H. H.; Olvera, J. M.; Wasiak, A.; Sajkiewicz, P. Polymer 2001, 42, 7153.
6. Wu, J.; Schultz, J. M.; Samon, J. M.; Pangelinan, A. B.; Chuah, H. H. Polymer 2001, 42, 7161.
7. Wu, G.; Li, H. W.; Wu, Y. Q.; John, A. C. Polymer 2002, 43, 4915.

8. Shu, Y. C.; Hsiao, K. J. Eur Polym J 2006, 42, 2773.
9. Ho, R. M.; Ke, K. Z.; Chen, M. Macromolecules 2000, 33, 7529.
10. Wang, B. J.; Christopher, Y. L.; Jennifer, H.; Stephen, Z. D. C.; Phillip, H. G. Polymer 2001, 42, 7171.
11. Chen, M.; Chen, C. C.; Ke, K. Z.; Ho, R. M. J Macromol Sci Phys 2002, 41, 1063.
12. Yun, J. H.; Kuboyama, K.; Chiba T.; Ougizawa, T. Polymer 2006, 47, 4831.
13. Chung, W. T.; Yeh, W. J.; Hong, P. D. J Appl Polym Sci 2002, 83, 2426.
14. Chuah, H. H. Polym Eng Sci 2001, 41, 308.
15. Hong, P. D.; Chung, W. T.; Hsu, C. F. Polymer 2002, 43, 3335.
16. Srimoaon, P.; Dangseeyun, N.; Supaphol, P. Eur Polym J 2004, 40, 599.
17. Chuang, W. T.; Hong, P. D.; Chuah, H. H. Polymer 2004, 45, 2413.
18. Xue, M. L.; Yu, Y. L.; Sheng, J.; Chuah, H. H. J Macromol Sci Polym Phys 2005, 44, 531.
19. Xue, M. L.; Sheng, J.; Yu, Y. L.; Chuah, H.H. Eur Polym J 2004, 40, 811.
20. Liu, Z.; Chen, K.; Yau, D. Eur Polym J 2003, 39, 2359.
21. Ou, C. F. J Polym Sci Part B: Polym Phys 2003, 41, 2902.
22. Liu, Z.; Chen, K.; Yau, D. Polym Test 2004, 23, 323.
23. Mishra, J. K.; Chang, Y. W.; Choi, N. S. Polym Eng Sci 2007, 47, 863.
24. Xu, Y.; Jia, H. B.; Piao, J. N.; Ye, S. R.; Huang, J. J Mater Sci 2008, 43, 417.
25. Chung, G. S.; Choi, K. R.; Lin, K. Y.; Kim, B. C. Polym Mater Sci Eng 2001, 84, 501.
26. Kuo, Y. H.; Woo, E. M. Polym J 2003, 35, 236.
27. Supaphol, P.; Dangseeyun, N.; Thanomkiat, P.; Nithitanakul, M. J Polym Sci B: Phys Ed 2004, 42, 676.
28. Supaphol, P.; Dangseeyun, N.; Srimoaon, P.; Nithitanakul, M. Polym Test 2004, 23, 175.
29. Xue, M. L.; Sheng, J.; Chuah, H. H.; Zhang, X. Y. J Macromol Sci Phys 2004, 43, 1045.
30. Lee, L. T.; Woo, E. M. Colloid Polym Sci 2004, 282, 1308.
31. Oh, S. J.; Chae, D. W.; Lee, H. J.; Kim, B. C. Polym Mater Sci Eng 2001, 84, 621.
32. Bae, W. J.; Jo, W. H.; Park, Y. H. Macromol Res 2002, 10, 145.
33. Ravikumar, H. B.; Raganathaiah, C.; Kumaraswamy, G. N.; Thomas, S. Polymer 2005, 46, 2372.
34. Aravind, I.; Albert, P.; Ranganathaia, C.; Kurian, J. V.; Thomas, S. Polymer 2005, 45, 4925.
35. Ravikumar, H. B.; Ranganathaiah, C. Polym Int 2005, 54, 1288.
36. Jafari, S. H.; Asadinezhad, A.; Yavari, A.; Khonakdar, H. A.; Bohme, F. Polym Bull 2005, 54, 417.
37. Jafari, S. H.; Yavari, A.; Asadinezhad, A.; Khonakdar, H. A.; Bohme, F. Polymer 2005, 46, 5082.
38. Kuo, J. M.; Woo, E. M.; Kuo, T. Y. Polym J 2001, 33, 920.
39. Huang, J. M.; Chang, F. C. J Appl Polym Sci 2002, 84, 850.
40. Fukunaga, K.; Maeno, T. J Electrostat 1997, 40/41, 431.
41. Kobayashi, T.; Wood, B. A.; Takemura, A.; Ono, H. J Electrostat 2006, 64, 377.
42. Kobayashi, T.; Wood, B. A.; Takemura, A.; Ono, H. Polym Eng Sci 2008, 48, 2247.
43. Kobayashi, T.; Wood, B., Takemura, A. J Appl Polym Sci 2011, 119, 2714.
44. Kobayashi, T.; Wood, B.; Blackman, G.; Takemura, A. J Appl Polym Sci 2011, 120, 3519.
45. Chang, J. C.; Kurian, J. V.; Miller, R. W. U.S. Pat.7,033,530 (2006).
46. Giardino, C. J.; Griffith, D. B.; Ho, C.; Howell, J. M.; Watkins, M. H.; Duffy, J. J. U.S. Pat. 6,353,062 (2002).
47. Zhang, J. J Appl Polym Sci 2004, 91, 1657.
48. Pyda, M.; Boller, A.; Grebowicz, J.; Chuah, H.; Lebedev, B. V.; Wunderlich, B. J Polym Sci Part B: Polym Phys 1998, 36, 2499.
49. Aravind, I.; Ahn, K. H.; Ranganathaiah, C.; Thomas, S. Ind Eng Chem Res 2009, 48, 9942.
50. Yavari, A.; Asadinezhad, A.; Jafari, S. H.; Khonakdar, H. A.; Bohme, F.; Hassler, R. Eur Polym J 2005, 41, 2880.
51. Zhang, Z., Xie, Y., Ma, D. Eur Polym J 1961 2001, 37.
52. Dlimoy, D., Goffaux, B.; Devaux, J., Legras, R. Polymer 1995, 36, 3255.
53. Gonzalez, C. C.; Perena, J. M.; Bello, A. J Polym Sci Part B: Polym Phys Ed 1988, 26, 1397.
54. Kalakkunnath, S.; Kalika, D. S. Polymer 2006, 47, 7085.
55. Mackintosh, A. R.; Liggat, J. J. J Appl Polym Sci 2004, 92, 2791.
56. Maxwell, A. S.; Monnerie, L.; Ward, I. M. Polymer 1998, 39, 6851.
57. Corrales, T.; Peinado, C.; Bosch, P.; Catalina, F. Polymer 2004, 45, 1545.
58. Couchman, P. R.; Karasz, F. E. Macromolecules 1978, 11, 117.
59. Fox, T. G. Bull Am Phys Soc 1956, 2, 123.
60. Gordon, M.; Taylor, J. S. J Appl Chem 1952, 2, 493.
61. Utracki, L. A. Adv Polym Technol 1985, 5, 33.
62. Aravind, I.; Eichhorn, K.; Komber, H.; Jehnichen, D.; Zafeiropulos, N. E.; Ahn, K. H.; Grohens, Y.; Stamm, M.; Thomas, S. J Phys Chem B 2009, 113, 1569.
63. Liu, W.; Mohanty, A. K.; Drzal, L. T.; Misra, M.; Kurian, J. V.; Miller, R.; Strickland, N. Ind Eng Chem Res 2005, 44, 857.
64. Shafee, E. E.; Zaki, M.; Saad, G. R. J Polym Res 2009, 16, 317.
65. Chiu, F. C.; Ting, M. H. Polym Test 2007, 26, 338.
66. Matsui, M.; Kashiwamura, T. Sen-I Gakkaishi 1993, 49, 421.